SMART assembly of congested C(sp^3)-rich architectures by iron-catalyzed conjunctive alkylation

Tong-De Tan[1,2], Juan M. I. Serviano[3], Xiaohua Luo[1], Peng-Cheng Qian[2], Patrick L. Holland[3,5], Xinglong Zhang[4,5] & Ming Joo Koh[1,5]

[1]Department of Chemistry, National University of Singapore, 4 Science Drive 2, Republic of Singapore, 117544.
[2]Institute of New Materials & Industry Technology, College of Chemistry & Materials Engineering, Wenzhou University, Wenzhou 325035, China.
[3]Department of Chemistry, Yale University, 225 Prospect Street, New Haven, Connecticut 06520, United States.
[4]Institute of High-Performance Computing, Agency for Science, Technology and Research (A∗STAR), 1 Fusionopolis Way, #16-16 Connexis, Republic of Singapore, 138632.
[5]These authors jointly supervised this work.
Corresponding author email: chmkmj@nus.edu.sg, zhang_xinglong@ihpc.a-star.edu.sg, patrick.holland@yale.edu

Catalytic cross-coupling by transition metals has revolutionized the formation of C–C bonds in organic synthesis. However, the challenge of forming multiple alkyl-alkyl bonds in crowded environments remains largely unresolved. Here, we report the regioselective functionalization of olefins with sp^3-hybridized organohalides and organozinc reagents using a simple (terpyridine)iron catalyst. Aliphatic groups of various sizes are successfully installed on either olefinic carbon, furnishing a diverse array of products with congested cores featuring C- or heteroatom-substituted stereocenters. The method enables access to valuable but synthetically challenging C(sp^3)-rich molecules, including alicyclic compounds bearing multiple contiguous stereocenters through annulation cascades. Mechanistic and theoretical studies suggest a stepwise metal-mediated alkyl radical transfer (SMART) pathway, which potentially opens the door to a broader scope of transformations and new chemical space.

sp^3-Centered carbon-carbon bonds form the cores of numerous biologically active natural products and their derivatives[1]. In particular, the number of saturated (sp^3) carbons correlates with solubility, suggesting that increased saturation leads to enhanced potency and selectivity in pharmaceuticals[2]. Therefore, developing methods for the expeditious construction of C(sp^3)-rich scaffolds has been a longstanding goal in organic synthesis. Although transition metal-catalyzed cross-coupling has become one of the most widely used synthetic tools to construct C–C bonds in the pharmaceutical industry[3], developments in this area are dominated by reactions involving sp^2 carbons (Fig. 1a). Compared to sp^2-hybridized substrates, the less-activated sp^3-hybridized variants are more resistant to oxidative addition during cross-coupling[4], and are also more

susceptible to undesired side reactions such as alkylmetal C_β-hydride elimination[5] which further complicate reaction systems. This inadvertently limits the chemical space accessible by synthetic and medicinal chemists, and consequently impacts the chemical and structural diversity of available drug-like compounds[6]. Given the greater difficulty of sp^3–sp^3 (alkyl-alkyl) cross-coupling[4,5], related catalytic processes are largely restricted to two-component reactions that form a single C–C bond[7-9]. Even then, forging a bond between sterically encumbered aliphatic groups (tertiary and secondary alkyl) to create congested stereocenters remains an onerous task[10] in synthetic chemistry. A catalytic process that assembles multiple alkyl-alkyl bonds to construct densely substituted entities would empower users to access medicinally valuable but synthetically elusive C(sp^3)-rich building blocks with sterically crowded stereocenters.

Three-component conjunctive cross-coupling reactions[11,12] are highly promising transformations capable of generating vicinal C(sp^3)–C(sp^3) linkages through dialkylation of easily accessible alkene precursors. However, there exist only a handful of regioselective dialkylation methods that afford non-congested adducts bearing tertiary carbon centers[13-18] with limited scope, and none involved the use of iron catalysis (Fig. 1b). In light of the low toxicity, low cost and high abundance of iron[19], there is compelling motivation to develop Fe-catalyzed conjunctive alkylation for sustainable organic synthesis[20]. However, this would require alkyliron intermediates that contain C_β–H bonds, which are viewed as unstable and susceptible to undesired C_β-hydride elimination[21] (Fig. 1c, top left). This partly explains why Fe-catalyzed olefin dialkylation remains a difficult and elusive transformation.

Bisphosphine-iron complexes were previously shown to mediate the union of certain olefins with activated haloalkanes and aryl or alkenyl Grignard reagents[22-24]. These reactions operate through radical cascades in which in situ-generated stabilized alkyl (*tert*-alkyl or fluoroalkyl) radicals undergo olefin addition prior to coupling with an organoiron species to facilitate C(sp^3)–C(sp^2) bond formation (Fig. 1c, top right). However, the requirement for dropwise addition (via syringe pump) of sensitive C(sp^2)-magnesium nucleophiles and activated alkyl halides as precursors of stabilized C-centered radicals somewhat limit the practicality and scope of products secured through this approach. Here, we report an Fe-catalyzed conjunctive alkylation cascade that forms multiple alkyl-alkyl bonds between olefins and two aliphatic reagents (dialkylzinc and haloalkane) of various substitution patterns and steric attributes (Fig. 1c, inset). Mechanistic and theoretical studies support a distinct mechanism consisting of an alkyl radical transfer step followed by alkylation. The present strategy suppresses C_β-hydride elimination of the alkyliron

intermediate, solving a common problem and paving the way to access saturated cyclic and acyclic molecules containing hindered C- or heteroatom-functionalized stereocenters.

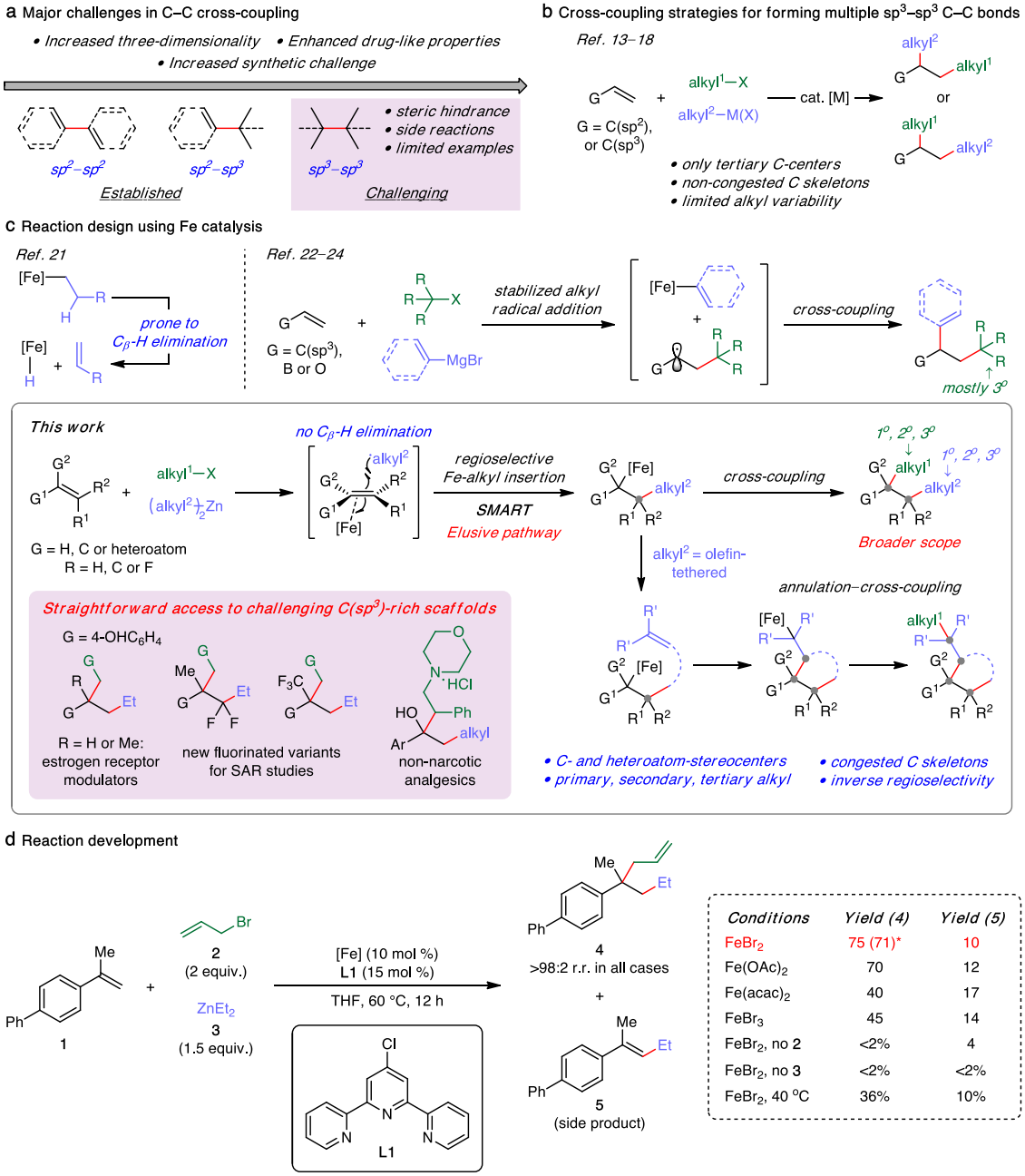

Fig. 1 | **Development of an iron-catalyzed strategy for conjunctive alkylation. a**, Challenges in constructing C–C bonds by cross-coupling. **b**, Previous catalytic approaches in conjunctive alkylation. X, halide; M, metal. **c**, Our design leveraging iron-catalyzed alkyl radical transfer–cross-coupling cascades to access complex C(sp^3)-rich building blocks. SMART, stepwise metal-mediated alkyl radical transfer; SAR, structure-activity relationship. **d**, Evaluation of reaction conditions (selected). Yields and regioisomeric ratios (r.r.) were determined by GC and ^{1}H NMR analysis. *Isolated yield.

Reaction development and mechanistic studies

Using 1,1-disubstituted alkene **1**, allyl bromide **2** (2 equiv.) and diethylzinc **3** (1.5 equiv.) as model substrates, we examined various reaction parameters for the multicomponent synthesis of **4** bearing a quaternary center (Tables S1–S6). In the presence of 10 mol % of the complex derived from $FeBr_2$ and terpyridine **L1** using THF as solvent at 60 °C for 12 hours, **4** was obtained exclusively as the sole regioisomer in 75% yield (71% isolated) (Fig. 1d). 10% of alkene **5**, presumably formed by undesired C_β-hydride elimination of the putative alkyliron intermediate (see Fig. 1c, inset), was also observed as a by-product. Notably, no side products arising from iron-hydride olefin addition were detected. Replacing $FeBr_2$ with other complexes such as $Fe(OAc)_2$, $Fe(acac)_2$ and $FeBr_3$ led to diminished yields of **4** and larger amounts of **5** (Table S1), and C_β-hydride elimination was more competitive under these conditions. Similar observations were detected when **L1** was changed to other tridentate or bidentate N-based ligands (Table S2). Lowering the temperature to 40 °C or switching the medium to other solvents (Table S3, S4) was detrimental to reaction efficiency. Excluding $FeBr_2$, **2** or **3** from the catalytic system led to <5% conversion of **1**. These results suggest that the reaction is unlikely to proceed through uncatalyzed carbozincation[25], and that **2** is necessary for catalytic turnover. Control experiments (Fig. S3) also revealed that the reaction is unlikely to occur by sequential Fe-catalyzed alkylzincation[26] followed by trapping with the electrophile[27].

Radical clock experiments were carried out to probe the plausible generation of carbon-centered radical species in our system (Fig. 2a). Ring cleavage to form **8** was detected when vinylcyclopropane **6** was subjected to standard dialkylation conditions, suggesting the intermediacy of a tertiary radical on the internal olefinic carbon. In a separate study, dialkylation using (2-(bromomethyl)cyclopropyl)benzene **9** predominantly led to the ring-ruptured product **11**. This indicates that the reaction likely proceeded via a cyclopropylmethyl radical, potentially obtained through Fe-mediated bromine atom abstraction[28], which is prone to ring opening to form a secondary benzylic radical[29]. Similar to the case in Fig. 1d, addition of **9** to the terminal olefinic carbon was minimal. In analogous fashion, the transformation with 1-hexene-derived dialkylzinc **13** resulted in a mixture of **14** and the cyclization adduct **15**. The formation of **15** could be rationalized by a putative 5-hexenyl radical intermediate undergoing annulation[30], implying that the olefin insertion step probably involved an Fe-catalyzed alkyl radical transfer pathway via an iron-alkyl complex.

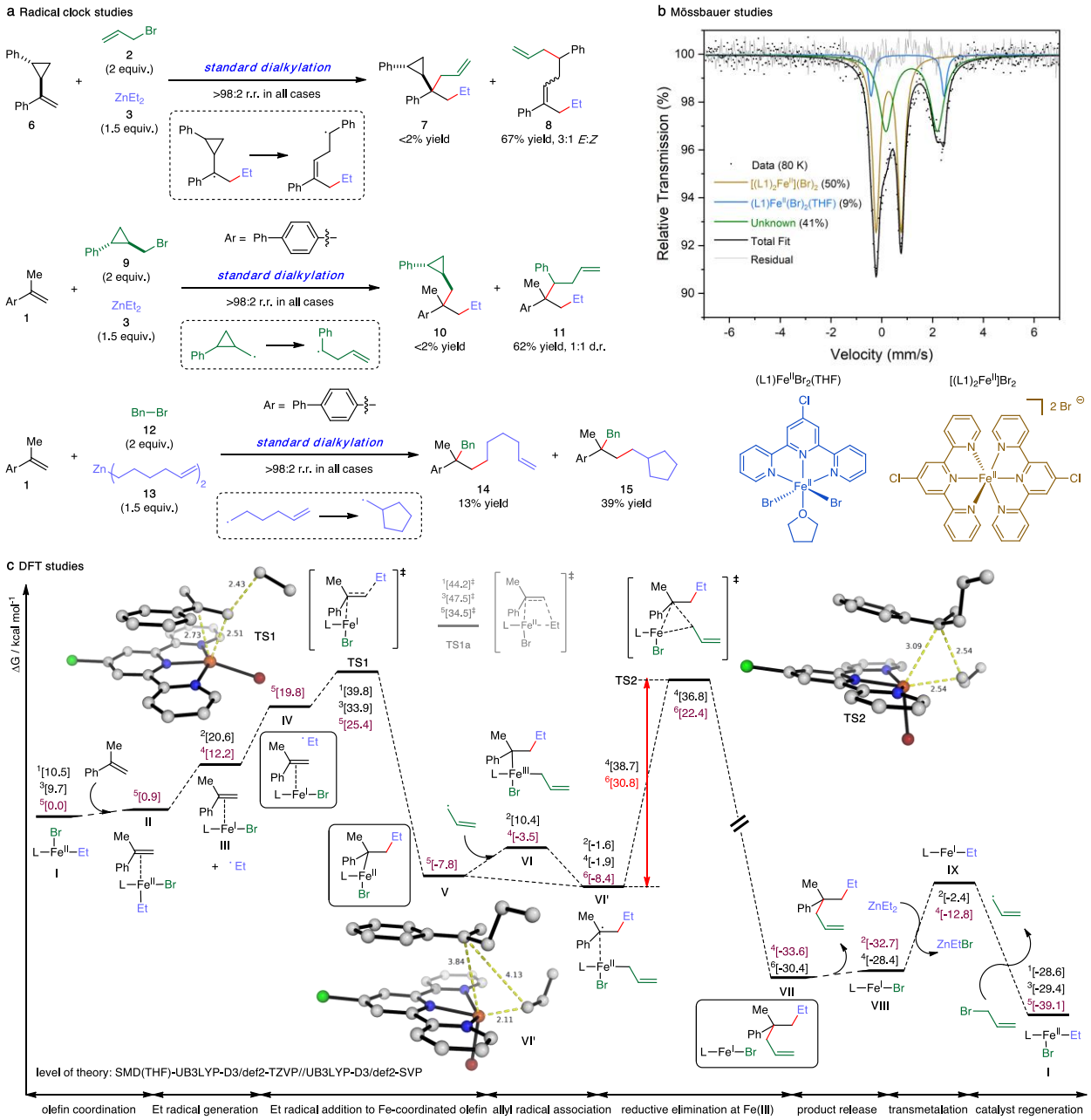

Fig. 2 | **Preliminary mechanistic investigations. a**, Radical clock experiments support the intermediacy of radical species derived from the olefin and alkylation reagents. **b**, Freeze-trapped 80 K Mössbauer spectra of the catalytic reaction using $^{57}FeBr_2$ after 3 h at 60 °C. **c**, Computed Gibbs energy profile for iron(II)-catalyzed conjunctive alkylation. Superscripts in front of energy values denote the spin states of the species. Key DFT optimized structures are shown with relevant bond distances given in Å. L, ligand **L1**; TS, transition state.

To identify the iron species present during catalysis, we probed the model reaction via ^{57}Fe Mössbauer spectroscopy (Fig. 2b). We performed the catalytic reaction with $^{57}FeBr_2$ and froze aliquots that were withdrawn at several time points. The Mössbauer spectra at 80 K all showed three species that accounted for all the observable iron. Two are assigned as [(**L1**)2Fe^{II}Br$_2$(THF)

and [(**L1**)Fe^{II}]Br_2, based on comparison to independently synthesized samples and literature data[31,32]. A third species has parameters that are close to those predicted from density functional theory (DFT) calculations on an optimized model of (**L1**)$Fe^{II}Br^{3-}$. None of the observed signals agreed with the parameters for literature (terpy)$Fe^{II}R_2$ complexes[33] or with DFT-predicted parameters for other potential alkyliron species (Table S8). These spectroscopic studies suggest that the major iron species in solution are iron(II) complexes that act as catalyst reservoirs, and that the catalytically active organoiron intermediates have very low concentrations. This situation is frequently found in organometallic catalysis, as highlighted by Halpern and others[34].

Since the catalytic intermediates were not detected, we used DFT calculations to assess the energetics of hypothetical catalytic mechanisms that are consistent with the mechanistic experiments described above. We compared pathways including various iron(I) and iron(II) intermediates (see supplementary information section 7), and found that those involving iron(I) species are kinetically incompetent (lowest energetic span[35] is 45.5 kcal/mol). The mechanism with reasonable barriers (Fig. 2c) begins with transmetalation of (**L1**)$Fe^{II}Br_2$ with diethylzinc **3** to form (**L1**)Fe^{II}BrEt (**I**). We considered a typical migratory insertion pathway in which I coordinates to the olefin and then the alkyl group inserts in a concerted step (transition state **TS1a**, Fig. 2c), but the barrier of 34.5 kcal/mol derived from **TS1a** is too high to explain the observed catalytic rate. Instead, the calculations show that olefin complexation weakens the Fe^{II}–Et bond from 21.3 kcal/mol to only 11.3 kcal/mol, leading to homolytic Fe–C cleavage that generates an ethyl radical. The ethyl radical presumably stays within the solvent cage and rapidly adds to the iron-coordinated C=C bond via transition state **TS1**, which is only 25.4 kcal/mol above **I**. This stepwise pathway has a much lower barrier than the concerted addition pathway, and we term it stepwise metal-mediated alkyl radical transfer (SMART).

SMART is regioselective for forming the tertiary alkyliron(II) intermediate, and the highly exergonic formation of the C(sp^3)–C(sp^3) bond affords the tertiary alkyliron complex **V**. This species can react with an allyl radical, generated by bromine atom abstraction from allyl bromide **2** by an organoiron species (see below) to give the unstable iron(III) complex **VI**. This complex is in equilibrium with **VI'** through reversible Fe–C bond homolysis. Spin density analysis suggests the presence of radical character on the tertiary carbon that reversibly forms the Fe^{III}–C bond (Fig. S30). This could account for the excellent site selectivity of SMART, because ethyl radical addition to the less substituted olefinic carbon delivers the more stabilized tertiary radicaloid intermediate. The ensuing reductive elimination occurs at the Fe^{III} center via transition state **TS2**

(barrier of 30.8 kcal/mol, Fig. 2c) to furnish the dialkylation product and a Fe^{I} species. Intrinsic reaction coordinates (IRC) connect **TS2** to complex **VI'** and **VII**, and show that as reductive elimination occurs, the Fe–C bond distance in **VI'** shortens, bringing the alkyl fragment closer to the iron center to facilitate C–C bond formation with the allyl group (see IRC movie). Generation of the second $C(sp^3)$–$C(sp^3)$ linkage is also exergonic and irreversible. The resulting (**L1**)Fe^{I}Br (**VIII**) then undergoes transmetalation with **3** to afford (**L1**)Fe^{I}Et (**IX**), which can subsequently abstract a bromine atom from **2** to regenerate **I** and allyl radical. The overall energetic span[35] of the computed catalytic cycle is 30.8 kcal/mol, which is compatible with the experimental observation of a reaction over 12 hours at 60 °C.

The proposed pathway for alkene insertion, SMART, is potentially enabling for a wider range of transformations and access to new chemical space. Although there are a number of applications for the homolysis of metal-carbon (M–C) bonds followed by addition of the alkyl radical to an olefin (for example, organometallic-mediated radical polymerization)[36], to our knowledge these studies have not considered the potential for pre-complexation of the olefin that induces M–C bond homolysis. Interestingly, SMART allows for less-stabilized primary alkyl radicals to undergo addition in a regiocontrolled manner, in contrast to existing Fe-catalyzed regimes that rely on the generation of stabilized alkyl radicals to promote reaction (**22**–**24**). It is also possible that the SMART pathway will be applicable for regioselective additions to other π-systems where weak M–C bonds could be involved[17]. Additionally, SMART opens the door to selective generation of multiple alkyl-alkyl bonds in sterically crowded environments, as shown below.

Scope of conjugative alkylation via SMART

We next evaluated the scope of the reaction using different classes of olefins (Fig. 3). A wide assortment of (hetero)aryl-functionalized alkenes served as effective substrates, furnishing the desired adducts containing quaternary (**17**–**29**) or tertiary (**16**, **30**) carbon centers with complete site selectivity. These include molecules bearing a silyl ether (**25**), a Lewis basic phthalimide (**26**), heteroarenes (**22**–**24**) as well as those derived from exocyclic olefins (**27**–**29**). Reaction of a 1,3-diene proceeded regioselectively at the less substituted terminus of the C=C bond (**30**). However, dialkylation with less reactive aliphatic olefins was found to be inefficient (**31**).

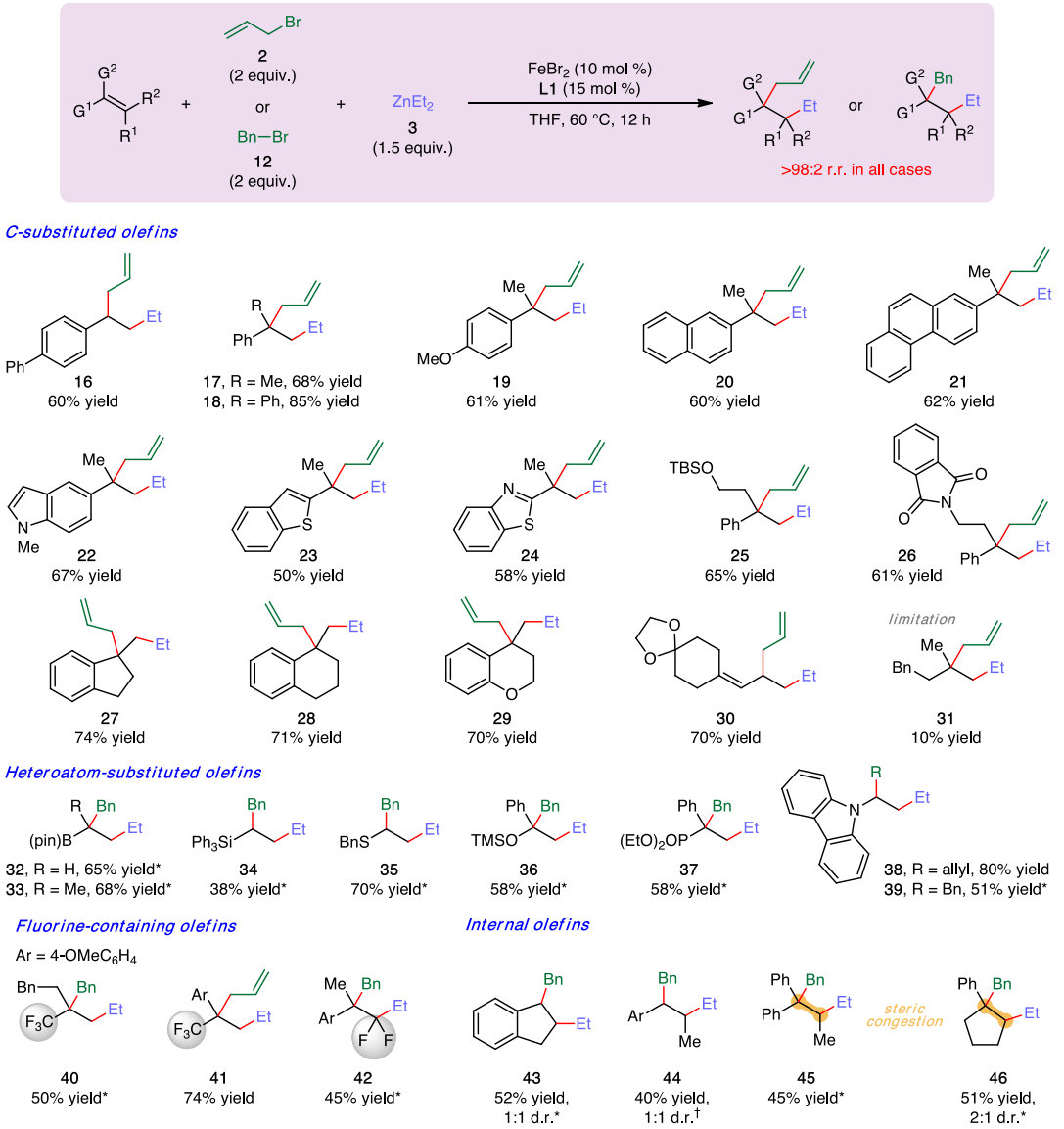

Fig. 3 | **Scope of olefins.** Unless otherwise stated, all products were obtained in >98:2 regioisomeric ratios. *Reaction was conducted with 10 mol % $Fe(OAc)_2$ and 15 mol % **L1** in DMA at 100 °C for 6 h. †Reaction was conducted with 20 mol % $Fe(OAc)_2$ and 30 mol % **L1** in DMA at 100 °C for 6 h.

Besides C-functionalized substrates, olefins appended to heteroatoms such as boron (**32**, **33**), silicon (**34**), sulfur (**35**), oxygen (**36**), phosphorus (**37**) and nitrogen (**38**, **39**) also participated in conjunctive alkylation, offering a distinct approach to synthetically valuable and/or biologically active entities carrying heteroatom-substituted stereocenters (**37**–**40**). It is worth mentioning that trifluoromethyl- and *gem*-difluoro-substituted C=C bonds underwent the desired reaction delivering medicinally important fluoroalkylated compounds (**40**–**42**)[41] without any trace of undesired defluorination from Cβ-fluoride elimination (**42**). Of particular note, the steric hindrance of internal olefins did not inhibit cross-coupling. Under standard conditions, endocyclic

and acyclic di- and trisubstituted alkenes were successfully converted to the corresponding dialkylated moieties (**43**–**46**), including examples that possess crowded sp^3–sp^3 carbon skeletons (**45**, **46**).

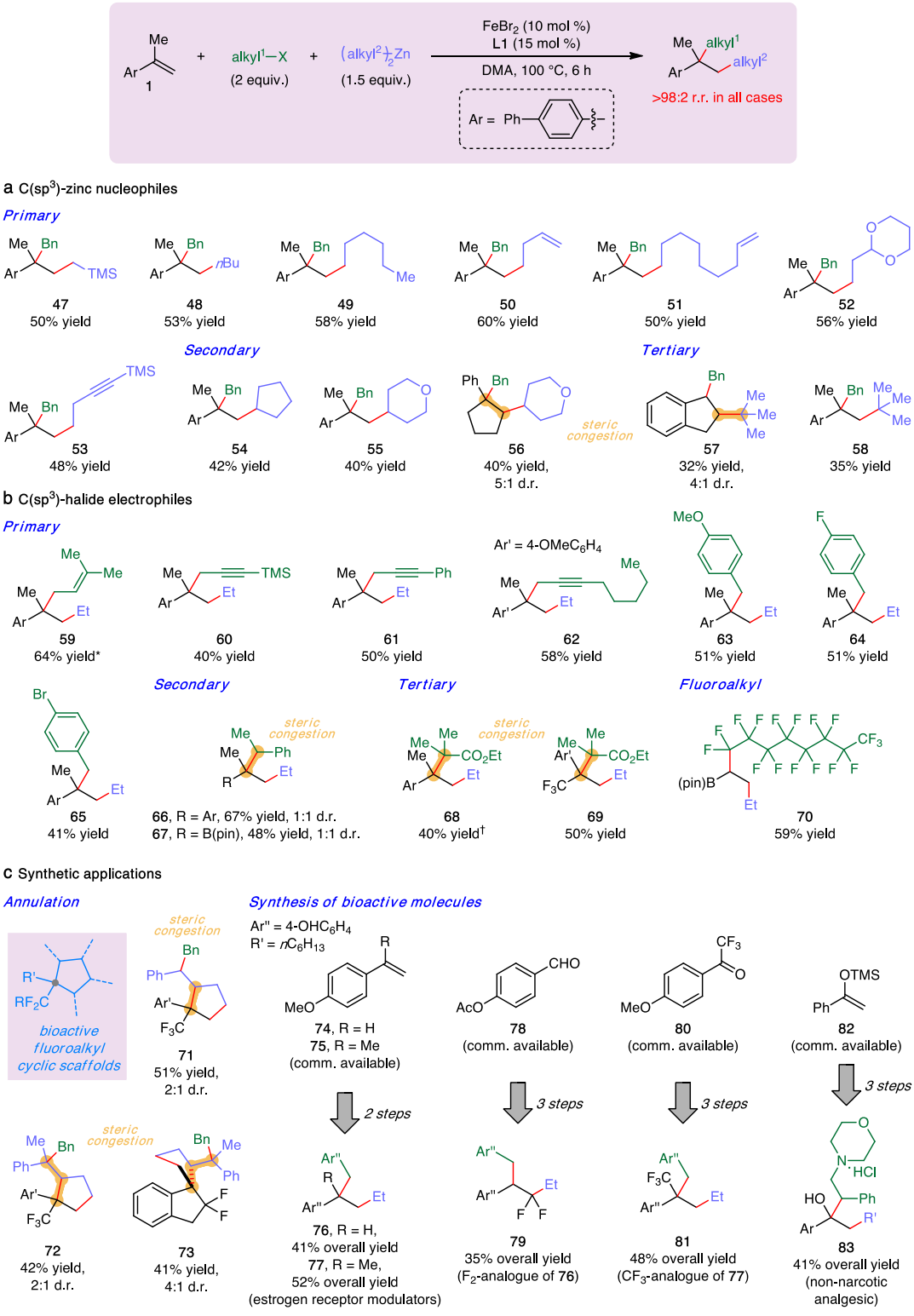

Fig. 4 | **Scope of dialkylation and synthetic utility. a**, Reactions with various dialkylzinc compounds. **b**, Reactions with various haloalkanes. **c**, Application to the synthesis of fluorinated annulation products and bioactive molecules. **83** was isolated as a single diastereomer. Unless otherwise stated, all products were obtained in >98:2 regioisomeric ratios. *Reaction was conducted in THF at 60 °C. †20 mol % $FeBr_2$ and 30 mol % **L1** were used.

A variety of aliphatic nucleophiles and electrophiles were explored to further probe the generality of the Fe-catalyzed transformation (Fig. 4). In DMA at 100 °C, dialkylzinc compounds with various electronic and steric properties were amenable to cross-coupling, enabling effective incorporation of primary (**47**–**53**), secondary (**54**–**56**) and tertiary (**57**, **58**) alkyl units to give the expected adducts as single regioisomers (Fig. 4a). Functional groups such as a silane (**47**), a terminal olefin, (**50**, **51**), an acetal (**52**), an alkyne (**53**) and a cyclic ether (**55**, **56**) are tolerated, and compounds with hindered alkyl-alkyl architectures (**56**, **57**) could be secured. Akin to the nucleophile scope, electronically and sterically varied organobromide(chloride) electrophiles underwent conjunctive alkylation (Fig. 4b). Among the primary aliphatic substrates tested, prenyl (**59**), propargyl (**60**–**62**) and benzyl (**63**–**65**) units could be successfully installed. However, long-chain alkyl bromides were insufficiently reactive in our system (Fig. S1). Nevertheless, this limitation may be circumvented by using the corresponding propargylated building blocks (**60**–**62**), and then using hydrogenation to obtain the fully saturated analogues.

Access to **59** is noteworthy given the crucial role of prenylation in protein-protein binding within biological systems[43]. Synthesis of **65** containing an aryl bromide moiety underscores the reaction's chemoselectivity, allowing for orthogonal functionalization if desired. Remarkably, the same regiochemical outcome was observed even in the presence of sterically demanding secondary (**66**, **67**), tertiary (**68**, **69**) and fluorous (**70**) bromoalkanes, which are known to generate stabilized radical species under transition metal catalysis (**11**, **22**–**24**) and trigger radical relay processes (see Fig. 1c, top right). In these cases, iron-alkyl insertion presumably outcompetes any adventitious formation/addition of the alkyl bromide-derived radical, and the observed sense of regioselectivity is opposite to those reported in the literature (**22**–**24**). The resulting product backbones comprise C–C bonds linking crowded tertiary-secondary and tertiary-tertiary alkyl motifs.

Synthetic applications

The observation of radical characteristics during the course of the reaction (see Fig. 2a) led us to hypothesize that intramolecular cyclization would give annulation products when the dialkylzinc included an olefin-tethered alkyl unit (see Fig. 1c). We evaluated the feasibility of a three-component annulation–cross-coupling cascade by reacting fluoroalkyl-substituted alkenes

with benzyl bromide and dialkylzinc compounds bearing pendant C=C bonds under standard conditions (Fig. 4c, left). Successful ring closure via 5-*exo* cyclization was achieved to afford sterically encumbered, fluorinated carbocycles **71**–**73** with up to three contiguous stereocenters, which may serve as precursors of medicinally relevant organofluorine scaffolds[44,45].

To further highlight utility, we employed the present Fe-catalyzed protocol as a key step for the concise synthesis of biologically active compounds (Fig. 4c, right). Subjecting the commercially available alkenes **74** and **75** to site-selective conjunctive alkylation and deprotection delivered estrogen receptor modulators **76** and **77**[46], respectively. Access to the *gem*-difluoro- and trifluoromethyl-substituted analogues **79** and **81**, which are potential candidates in structure-activity relationship studies[41] but non-trivial to synthesize, could be achieved in a straightforward fashion by employing the corresponding fluorinated olefin substrates. Preparation of non-narcotic analgesic **83**[47] was executed in three steps by dialkylation of commercially available enol silane **82** followed by deprotection and acidification. **83** was isolated in 41% overall yield as a single diastereomer after purification.

Conclusions

In summary, the catalytic method reported here provides a powerful and sustainable approach for assembling congested sp^3-hybridized carbon frameworks, which would potentially accelerate the synthesis of many natural products and pharmaceuticals featuring densely functionalized alkyl-alkyl linkages. The mechanistic insights are expected to unlock unexplored avenues for building molecular complexity and diversity through conjunctive cross-coupling reactions of readily available precursors.

Data availability

DFT optimized structures, relevant IRC and TS movies and Mulliken spin population analysis files have been uploaded to zenodo.org (DOI: 10.5281/zenodo.7336845). All other data are available in the main text or the supplementary information.

References

1 Geist, E., Kirschning, A. & Schmidt, T. sp^3-sp^3 Coupling reactions in the synthesis of natural products and biologically active molecules. *Natural Prod. Rep.* **31**, 441–448 (2014).

2 Lovering, F., Bikker, J. & Humblet, C. Escape from flatland: increasing saturation as an approach to improving clinical success. *J. Med. Chem.* **52**, 6752–6756 (2009).

3 de Meijere, A. & Diederich, F. *Metal-Catalyzed Cross-Coupling Reactions* (Wiley-VCH, 2004).

4 Kranthikumar, R. Recent advances in $C(sp^3)$–$C(sp^3)$ cross-coupling chemistry: a dominant performance of nickel catalysts. *Organometallics* **41**, 667–679 (2022).

5 Choi, J. & Fu, G. C. Transition metal-catalyzed alkyl-alkyl bond formation: Another dimension in cross-coupling chemistry. *Science* **356**, eaaf7230 (2017).

6 Blakemore, D. C. *et al.* Organic synthesis provides opportunities to transform drug discovery. *Nat. Chem.* **10**, 383–394 (2018).

7 Johnston, C. P., Smith, R. T., Allmendinger, S. & MacMillan, D. W. C. Metallaphotoredox-catalysed sp^3-sp^3 cross-coupling of carboxylic acids with alkyl halides. *Nature* **536**, 322–325 (2016).

8 Qin, T. *et al.* A general alkyl-alkyl cross-coupling enabled by redox-active esters and alkylzinc reagents. *Science* **352**, 801–805 (2016).

9 Zhang, W. *et al.* Electrochemically driven cross-electrophile coupling of alkyl halides. *Nature* **604**, 292–297 (2022).

10 Liu, W., Lavagnino, M. N., Gould, C. A., Alcazar, J. & MacMillan, D. W. C. A biomimetic S_H2 cross-coupling mechanism for quaternary sp^3-carbon formation. *Science* **374**, 1258–1263 (2021).

11 Wickham, L. & Giri, R. Transition metal (Ni, Cu, Pd)-catalyzed alkene dicarbofunctionalization reactions. *Acc. Chem. Res.* **54**, 3415–3437 (2021).

12 Zhang, L. *et al.* Catalytic conjunctive cross-coupling enabled by metal-induced metallate rearrangement. *Science* **351**, 70–74 (2016).

13 Dhungana, R. K. *et al.* Ni-catalyzed regioselective 1,2-dialkylation of alkenes enabled by the formation of two $C(sp^3)$–$C(sp^3)$ bonds. *J. Am. Chem. Soc.* **142**, 20930–20936 (2020).

14 Yang, T. *et al.* Chemoselective union of olefins, organohalides and redox-active esters enables regioselective alkene dialkylation. *J. Am. Chem. Soc.* **142**, 21410–21419 (2020).

15 Wang, X.-X., Lu, X., He, S.-J. & Fu, Y. Nickel-catalyzed three-component olefin reductive dicarbofunctionalization to access alkylborates. *Chem. Sci.* **11**, 7950–7956 (2020).

16 Terao, J., Saito, K., Nii, S., Kambe, N. & Sonoda, N. Regioselective double alkylation of styrenes with alkyl halides using a titanocene catalyst. *J. Am. Chem. Soc.* **120**, 11822–11823 (1998).

17 Mizutani, K., Shinokubo, H. & Oshima, K. Cobalt-catalyzed three-component coupling reaction of alkyl halides, 1,3-dienes, and trimethylsilylmethylmagnesium chloride. *Org. Lett.* **5**, 3959–3961 (2003).

18 Derosa, J., van der Puyl, V. A., Tran, V. T., Liu, M. & Engle, K. M. Directed nickel-catalyzed 1,2-dialkylation of alkenyl carbonyl compounds. *Chem. Sci.* **9**, 5278–5283 (2018).

19 Rana, S., Biswas, J. P., Paul, S., Paik, A. & Maiti, D. Organic synthesis with the most abundant transition metal-iron: from rust to multitasking catalysts. *Chem. Soc. Rev.* **50**, 243–472 (2021).

20 Piontek, A., Bisz, E. & Szostak, M. Iron-catalyzed cross-couplings in the synthesis of pharmaceuticals: in pursuit of sustainability. *Angew. Chem. Int. Ed.* **57**, 11116–11128 (2018).

21 Bellows, S. M., Cundari, T. R. & Holland, P. L. Spin crossover during β-hydride elimination in high-spin iron(II)- and cobalt(II)-alkyl complexes. *Organometallics* **32**, 4741–4751 (2013).

22 Liu, L. *et al.* General method for iron-catalyzed multicomponent radical cascades-cross-couplings. *Science* **374**, 432–439 (2021).

23 Liu, L. *et al.* Fe-catalyzed three-component dicarbofunctionalization of unactivated alkenes with Grignard reagents. *Chem. Sci.* **11**, 8301–8305 (2021).

24 Rotella, M. E., Sar, D., Liu, L. & Gutierrez, O. Fe-catalyzed dicarbofunctionalization of electron-rich alkenes with Grignard reagents and (fluoro)alkyl halides. *Chem. Commun.* **57**, 12508–12511 (2021).

25 Sklute, G., Cavender, H. & Marek, I. Carbozincation reactions of carbon-carbon multiple bonds. *Org. React.* **87**, 507–763 (2015).

26 Huang, Q. *et al.* Iron-catalyzed vinylzincation of terminal alkynes. *J. Am. Chem. Soc.* **144**, 515–526 (2022).

27 Zhang, C. *et al.* Enantiomerically enriched *α*-borylzinc reagents by nickel-catalyzed carbozincation of vinylboronic esters. *J. Am. Chem. Soc.* **143**, 14189–14195 (2021).

28 Ilies, L., Matsubara, T., Ichikawa, S., Asako, S. & Nakamura, E. Iron-catalyzed directed alkylation of aromatic and olefinic carboxamides with primary and secondary alkyl tosylates, mesylates, and halides. *J. Am. Chem. Soc.* **136**, 13126–13129 (2014).

29 Newcomb, M. in *Encyclopedia of Radicals in Chemistry, Biologyand Materials*, C. Chatgilialoglu and A. Studer, Eds. (Wiley, 2012).

30 Yi, X., Mao, R., Lavrencic, L. & Hu, X. Photocatalytic decarboxylative coupling of aliphatic N-hydroxyphthalimide esters with polyfluoroaryl nucleophiles. *Angew. Chem. Int. Ed.* **60**, 23557–23563 (2021).

31 Reiff, W. M., Erickson, N. E. & Baker Jr., W. A. Mono(2,2',2''-terpyridine) complexes of iron(II). *Inorg. Chem.* **8**, 2019–2021 (1969).

32 England, J., Scarborough, C. C., Weyhermüller, T., Sproules, S. & Wieghardt, K. Electronic structures of the electron transfer series $[M(bpy)_3]^n$, $[M(tpy)_2]^n$, and $[Fe(tbpy)_3]^n$ (M = Fe, Ru; n = 3+, 2+, 1+, 0, 1–): A Mössbauer spectroscopic and DFT study. *Eur. J. Inorg. Chem.* 4605–4621 (2012).

33 Tondreau, A. M. *et al.* Synthesis, electronic structure, and alkene hydrosilylation activity of terpyridine and bis(imino)pyridine iron dialkyl complexes. *Organometallics* **31**, 4886–4893 (2012).

34 Halpern, J. Mechanistic aspects of homogeneous catalytic hydrogenation and related processes. *Inorg. Chim. Acta* **50**, 11–19 (1981).

35 Kozuch, S. & Shaik, S. How to conceptualize catalytic cycles? The energetic span model. *Acc. Chem. Res.* **44**, 101–110 (2011).

36 Poli, R. New phenomena in organometallic-mediated radical polymerization (OMRP) and perspectives for control of less active monomers. *Chem. Eur. J.* **21**, 6988–7001 (2015).

37 Franz, A. K. & Wilson, S. O. Organosilicon molecules with medicinal applications. *J. Med. Chem.* **56**, 388–405 (2013).

38 Vitaku, E., Smith, D. T. & Njardarson, J. T. Analysis of the structural diversity, substitution patterns, and frequency of nitrogen heterocycles among U.S. FDA approved pharmaceuticals. *J. Med. Chem.* **57**, 10257–10274 (2014).

39 Baker, S. J. *et al.* Therapeutic potential of boron-containing compounds. *Future Med. Chem.* **1**, 1275–1288 (2009).

40 Shennan, B. D. A. *et al.* Branching out: redox strategies towards the synthesis of acyclic α-tertiary ethers. *Chem. Soc. Rev.* **51**, 5878–5929 (2022).

41 Hagmann, W. K. The many roles for fluorine in medicinal chemistry. *J. Med. Chem.* **51**, 4359–4369 (2008).

42 Fujita, T., Fuchibe, K. & Ichikawa, J. Transition-metal-mediated and -catalyzed C−F bond

activation by fluorine elimination. *Angew. Chem. Int. Ed.* **58**, 390–402 (2019).
43 Wang, M. & Casey, P. J. Protein prenylation: unique fats make their mark on biology. *Nat. Rev. Mol. Cell Biol.* **17**, 110–122 (2016).
44 Iakovenko, R. O. *et al.* Reactions of CF_3-enones with arenes under superelectrophilic activation: a pathway to *trans*-1,3-diaryl-1-CF_3-indanes, new cannabinoid receptor ligands. *Org. Biomol. Chem.* **13**, 8827–8842 (2015).
45 Begue, J. P. & Bonnet-Delpon, D. *Bioorganic and Medicinal Chemistry of Fluorine.* (Wiley, Hoboken, 2008).
46 Waibel, M. *et al.* Bibenzyl- and stilbene-core compounds with non-polar linker atom substituents as selective ligands for estrogen receptor beta. *Eur. J. Med. Chem.* **44**, 3412–3424 (2009).
47 Gasparyan, N. K., Gevorgyan, G. A., Paronikyan, R. G., Tumadzhyan, A. E. & Panosyan, G. A. Synthesis and biological activity of diaryl-substituted 3-morpholinopropanols. *Pharm. Chem. J.* **39**, 361–363 (2005).

Acknowledgements

X.Z. acknowledges the A*STAR Computational Resource Centre (A*CRC) of Singapore for the partial use of its high-performance computing facilities. Funding: This research was supported by the Ministry of Education of Singapore Academic Research Fund Tier 2: A-8000034-00-00 (M.J.K.), the Foundation of Wenzhou Science & Technology Bureau: No. ZY2020027 (T.-D.T. and P.-C.Q.), the Institute of High Performance Computing and the Deputy Chief Executive Research Office (DCERO) A*STAR Career Development Fund: C210812008 (X.Z.) and the National Institutes of Health: GM129081 (P.L.H.).

Author contributions

M.J.K. and T.-D.T. conceived the project. T.-D.T., X.L. and P.-C.Q. developed the catalytic method. J.M.I.S. and P.L.H. designed and performed the Mössbauer studies. X.Z. designed and performed the DFT studies. All authors contributed to the writing of the manuscript.

Competing interests

The authors declare no competing interests.

Additional information

Supplementary Information is available for this paper at...

Reprints and permissions information is available at www.nature.com/reprints.

Correspondence and requests for materials should be addressed to M.J.K. (chmkmj@nus.edu.sg), X.Z. (zhang_xinglong@ihpc.a-star.edu.sg) and P.L.H. (patrick.holland@yale.edu).